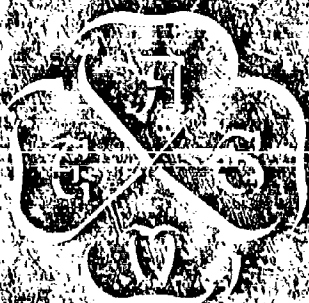


AD-A285 286



AN  
**ASME**  
PUBLICATION



FOR ASME MEMBERS

The Society shall not be responsible for statements or opinions advanced in papers or in discussion at meetings of the Society or of its Divisions or Sections or printed in its publications.

Discussion is printed only if the paper is published in an ASME journal.

THE AMERICAN SOCIETY OF MECHANICAL ENGINEERS  
29 West 39th Street, New York 18, N. Y.

PAPER NUMBER

N96369X

61-WA-37



COPY 1

# A Study of Axial-Flow Turbine Efficiency Characteristics in Terms of Velocity Diagram Parameters

WARNER L. STEWART

Head, Turbodrives Section,  
Lewis Research Center, National  
Aeronautics and Space Administration,  
Cleveland, Ohio.

This document has been approved for public release and sale; its distribution is unlimited.

This paper presents the results of a study aimed at providing a systematic method of rapidly estimating turbine efficiency level for a selected set of velocity diagrams. The development of the method utilizes certain basic concepts described previously in ASME and NASA publications by the author, in relating the blade-loss characteristics to the turbine mean-section velocity diagrams. The basic diagram parameter used in the development is a speed work parameter, defined as the ratio of mean-section blade speed squared to the over-all specific work output. Other factors considered in the development include number of turbine stages, stator-exit angle, Reynolds number, and leaving loss. The results of the analysis include a parametric study of the effect of these variables on efficiency as well as a comparison of the performance predicted by the method with that obtained experimentally.

LIBRARY COPY

SEP 1962

94-29127



on for presentation at the Winter Annual Meeting, New York, N. Y., November 26-December 1, 1961, of The American Society of Mechanical Engineers. Manuscript received at ASME Headquarters, June 16, 1961.

Written discussion on this paper will be accepted up to January 10, 1962.

Copies will be available until October 1, 1962.

# A Study of Axial-Flow Turbine Efficiency Characteristics in Terms of Velocity Diagram Parameters

WARNER L. STEWART

The aerodynamic design of axial-flow turbines, in general, can be divided into three phases. The first phase is the selection of the over-all requirements of the turbine and includes fluid used, temperature and pressure levels, flow rate, power level, rotative speed, and perhaps a required efficiency level. The second phase is the determination of the turbine geometry that best meets these requirements. The results of this phase would be the determination of the number of turbine stages, turbine and blading sizing, blade turning, and rate of expansion through the turbine. The general method of executing the second phase is through the calculation of the velocity diagrams in the free-stream region before and after each blade row. The third phase is then the evolution of the blade shapes that will meet the velocity-diagram requirements and should involve the use of three-dimensional design procedures to obtain the surface velocity distributions (1)<sup>1</sup> and the exercising of diffusion controls upon these distributions (2).

The expected efficiency of the turbine that is evolved to meet the requirements set up in the first phase depends upon both the over-all geometry selected in phase two and the detailed blading design in phase three. The level of efficiency expected is a function of the second phase through the aerodynamic severity of the selected velocity diagram. The additional effect of the third phase on efficiency occurs as a result of its sensitivity to such blade and mechanical design features as surface loading, trailing-edge blockages, and tip and running clearances.

This paper presents a method of estimating the level of efficiency as a function of the selected velocity diagrams that are needed in conducting phase two. The basic parameter used is a speed-work parameter  $\lambda$ , defined as the ratio of the mean-section blade speed squared to the specific work output. This parameter is similar to the familiar "Larson's Characteristic Number" described in (3). Other factors affect-

ing the efficiency level and included in the development are the number of turbine stages, stator-exit angle, Reynolds number, and turbine-exit axial component of velocity head. Included in the paper will be the development of the required equations, application of the equations to show the effect of these variables on efficiency, and finally a comparison with some available experimental results.

## NOMENCLATURE

- A = blade-loss term defined by equation (21a)
- B = stage leaving-loss term defined by equation (21b)
- C = parameter defined by equation (24a)
- D = parameter defined by equation (24b)
- k = parameter defined by equation (33)
- g = acceleration due to gravity, 32.17 ft/sec<sup>2</sup>
- h = specific enthalpy, Btu/lb
- J = mechanical equivalent of heat, 778.2 ft-lb/Btu
- K = constant of proportionality, equation (23)
- L = blade kinetic-energy losses defined by equations (19) and (20)
- l = blade height, ft
- N = number of turbine stages
- Re = Reynolds number defined by equation (31)
- r = mean-section radius, ft
- U = mean-section blade speed, fps
- V = absolute gas velocity, fps
- W = relative gas velocity, fps
- w = weight-flow rate, lb/sec
- $\alpha$  = stator angle measured from axial direction, deg
- $\beta$  = rotor angle measured from axial direction, deg
- $\eta$  = adiabatic efficiency based on total to total-pressure ratio
- $\eta_s$  = adiabatic efficiency based on total to static-pressure ratio
- $\lambda$  = speed-work parameter,  $U^2/gJA$
- $\mu$  = gas viscosity, lb/(ft)(sec)
- $\nu$  = blade-jet speed ratio
- $\rho$  = gas density, lbf

<sup>1</sup> Underlined numbers in parentheses designate References at the end of the paper.

A-1

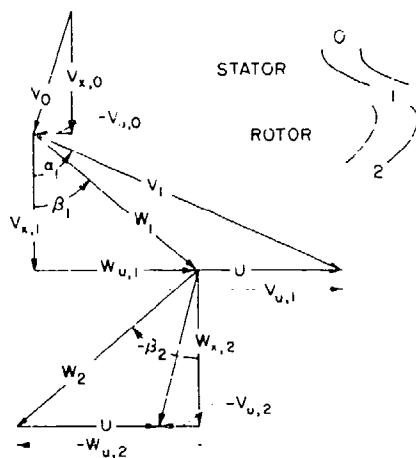


Fig. 1 Typical turbine-stage velocity diagrams showing nomenclature used

#### Subscripts

- a = first stage
- i = intermediate stage
- id = ideal
- j = denoting jet velocity as defined by equation (10)
- l = last stage
- ro = rotor
- s = based on total to static conditions across stage or turbine
- st = stator
- u = tangential component
- x = axial component
- 0 = station upstream of stage
- 1 = station between stator and rotor
- 2 = station downstream of stage

#### Superscripts

- ' = absolute total state
- = over-all

#### DEVELOPMENT

##### Speed-Work Parameter

As pointed out in the introduction, the speed-work parameter  $\lambda$  is used as the basic parameter in relating the efficiency to the velocity-diagram parameters. For a stage this parameter is defined as

$$\lambda = \frac{U^2}{gJ \Delta h'} \quad (1)$$

and can be considered as the ratio of the energy associated with the mean-section blade speed to the stage specific work output. Since the stage specific work output can be written in terms of velocity diagram quantities as

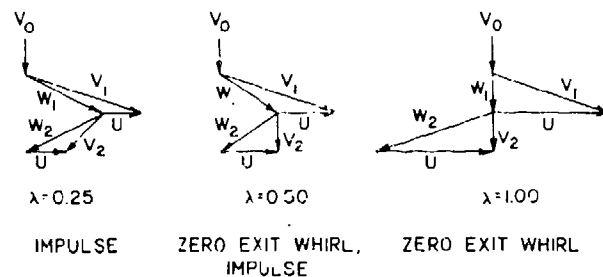


Fig. 2 Turbine velocity-diagram types used as a function of speed-work parameter,  $\lambda$

$$\Delta h' = \frac{U \Delta V_u}{gJ} \quad (2)$$

Another expression for  $\lambda$  can be obtained as

$$\lambda = \frac{U}{\Delta V_u} \quad (3)$$

Equation (3) shows that  $\lambda$  is a measure of the severity of the stage velocity diagram in terms of the relation of the blade speed to change in tangential momentum. Fig. 1 presents a typical set of stage-velocity diagrams showing the symbols and station nomenclature used. The whirl parameter  $\Delta V_u$  can be related to the absolute tangential velocities at the rotor entrance and exit by the following equation:

$$\Delta V_u = V_{u,1} - V_{u,2} \quad (4)$$

Using equation (2) in (1) a different way yields a third equation for  $\lambda$  as

$$\lambda = \frac{gJ \Delta h'}{\Delta V_u^2} \quad (5)$$

This equation is used later in the development.

For axial-flow turbines the value of  $\lambda$  varies normally from 0 to 1.00. As the parameter is varied over this range, the associated type of velocity diagram also changes. These types are illustrated in Fig. 2 where velocity diagrams for three values of  $\lambda$ , 0.25, 0.50, and 1.00, are shown. A  $\lambda$  value of unity results in  $\Delta V_u = U$ . The velocity diagram used for this value generally utilizes reaction or a velocity increase across both stator and rotor with zero exit whirl. As  $\lambda$  is reduced, zero exit whirl is maintained with, however, the reaction in the rotor decreasing until at  $\lambda = 0.50$  impulse conditions are reached. In this paper impulse conditions are defined to occur when

$$W_{u,1} = W_{u,2} \quad (6)$$

and approximates the more familiar connotation of impulse as a constant static pressure across the blade row.

References such as (2) have shown marked increases in blade loss as negative reaction is imposed. Therefore a limit on reaction of zero (impulse conditions) is imposed on every blade row. In view of this limitation, at values of  $\lambda$  below 0.50 the rotor is specified to operate at impulse with a subsequent requirement of negative whirl at the stage exit. Over the entire range of  $\lambda$  then the stage tangential velocities (ratioed to the total change in whirl  $\Delta V_u$ ) can be written as

$$0 \leq \lambda \leq 0.50$$

$$\frac{V_{u,1}}{\Delta V_u} = \lambda + \frac{1}{2} \quad (7a)$$

$$\frac{V_{u,2}}{\Delta V_u} = \lambda - \frac{1}{2} \quad (7b)$$

$$0.50 \leq \lambda \leq 1.00$$

$$\frac{V_{u,1}}{\Delta V_u} = 1 \quad (7c)$$

$$\frac{V_{u,2}}{\Delta V_u} = 0 \quad (7d)$$

In the general case of the multistage turbine, it is assumed that the mean-section blade speed  $U$  is the same for all stages (constant mean-section diameter), and each stage puts out an equal amount of work. Therefore by defining  $\bar{\lambda}$  as the over-all speed-work parameter of the turbine, a relation with  $\lambda$  can be obtained as

$$\bar{\lambda} = \frac{U^2}{gJ \Delta h'} = \frac{U^2}{NgJ \Delta h'} \frac{\lambda}{N} \quad (8)$$

Another parameter often used in describing turbine efficiency is the blade-jet speed ratio. This parameter  $\bar{v}$  is defined as the ratio of the mean-section blade speed to the jet velocity corresponding to the ideal expansion from inlet total to exit static conditions across the turbine. That is

$$\bar{v} = \frac{U}{V_j} \quad (9)$$

where

$$\frac{V_{j,1}^2}{2gJ} = \Delta h_{1d,s} \quad (10)$$

A relation between  $\bar{v}$  and  $\bar{\lambda}$  can be obtained by use of equations (8) to (10) together with the equation for static efficiency

$$\bar{\eta}_s = \frac{\Delta h'}{\Delta h_{1d,s}} \quad (11)$$

The resultant relation is

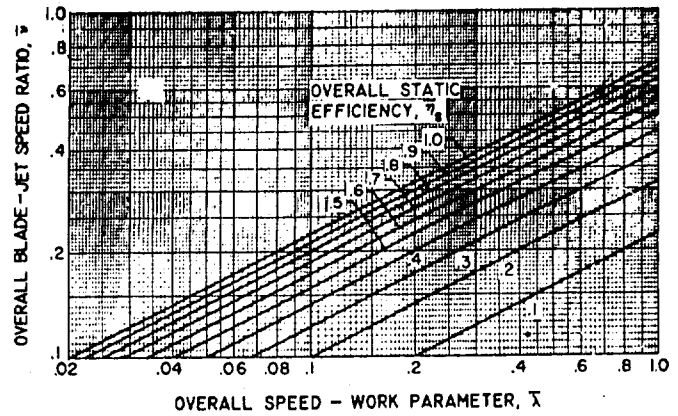


Fig.3 Graphical relation between blade-jet speed ratio and speed-work parameter

$$\bar{v} = \left( \frac{\bar{\eta}_s \bar{\lambda}}{2} \right)^{\frac{1}{2}} \quad (12)$$

which shows the two parameters related by the static efficiency. Therefore, if efficiency is a function of one of these parameters, it must also be a function of the other. The parameter  $\lambda$  is used herein as it is related directly to the actual velocity diagram whereas  $\bar{v}$  is not. The relation between  $\bar{v}$  and  $\bar{\lambda}$  is shown graphically in Fig.3.

#### Relation Between Speed-Work Parameter and Efficiency

Two types of stage efficiency will be used in this paper. The first, total efficiency  $\eta$ , is defined as the ratio of the actual stage specific work output divided by the ideal specific work output corresponding to the total to total-pressure ratio across the stage. That is,

$$\eta = \frac{\Delta h'}{\Delta h_{1d}} \quad (13)$$

The second type is the static efficiency  $\eta_s$ , defined the same as the total efficiency except that the ideal stage specific work output corresponds to the total to static-pressure ratio across the stage. In equation form:

$$\eta_s = \frac{\Delta h'}{\Delta h_{1d,s}} \quad (14)$$

When multistaging is considered in this paper, an over-all static efficiency  $\bar{\eta}_s$  will also be used. The relation between this efficiency and the stage values can be obtained considering that the stage specific work outputs are the same. Thus,

$$\bar{\eta}_s = \frac{N \Delta h'}{\Delta h_{1d,s}} \quad (15)$$

Any effect of reheat within the turbine is neglected in order that the equations developed are independent of enthalpy level. This effect is also relatively small. In view of this assumption  $\Delta h_{id,s}$  can be equated to the sum of those occurring across each stage; that is,

$$\Delta h_{id,s} = \Delta h_{id,a} + (N - 2) \Delta h_{id,1} + \Delta h_{id,l,s} \quad (16)$$

where  $a$  represents the first stage,  $1$  and intermediate stage, and  $l$  the last stage. The difference in the ideal specific work among these stages occurs because, since constant work per stage is specified, the intermediate and last stage will differ from the first in terms of the stator geometry and associated loss, and then, of course, the last stage including the turbine exit leaving loss.

Substituting equation (16) into (15) and dividing through by  $\Delta h'$  yields

$$\bar{\eta}_s = \frac{N}{\frac{1}{\eta_a} + \frac{N-2}{\eta_1} + \frac{1}{\eta_{l,s}}} \quad (17)$$

Consideration of the relation between the speed-work parameter and efficiency will be made using the stage efficiency  $\eta_s$ . The equation for  $\eta$  is the same except for the deletion of the stage exit kinetic energy loss term. Neglecting reheat effects as described above, the ideal stage specific work output can be written as

$$\Delta h_{id,s} = \Delta h' + L_{st} + L_{ro} + \frac{v_2^2}{2gJ} \quad (18)$$

where

$$\frac{v_2^2}{2gJ} = \text{leaving loss}$$

$L_{st}$  = kinetic energy loss across stator

$$L_{st} = \frac{v_{id,1}^2}{2gJ} - \frac{v_1^2}{2gJ} \quad (19)$$

$L_{ro}$  = kinetic energy loss across rotor

$$L_{ro} = \frac{w_{id,2}^2}{2gJ} - \frac{w_2^2}{2gJ} \quad (20)$$

See appendix C of (4) to verify equation (18).

Substituting equation (18) into equation (14) yields

$$\eta_s = \frac{\Delta h'}{\Delta h' + L_{st} + L_{ro} + \frac{v_2^2}{2gJ}}$$

Dividing through by  $\Delta V_u^2$  and using equation (5) yield

$$\eta_s = \frac{\lambda}{\lambda + \frac{1}{2}(A + B)} \quad (21)$$

where

$$A = \frac{2gJ(L_{st} + L_{ro})}{\Delta V_u^2} \quad (21a)$$

$$B = \left( \frac{v_2}{\Delta V_u} \right)^2 \quad (21b)$$

To obtain  $\eta$ , the term  $B$  is not used. The relation between terms  $A$  and  $B$  and the diagram parameters of interest must now be obtained.

#### Consideration of Blade-Loss Term A

The term  $A$  represents the contribution of the blade losses to the stage inefficiency. These losses are assumed to be proportional to the following:

(a) Reynolds number to the  $-1/5$  power. This assumption represents the normal manner in which the loss is assumed to vary with Reynolds number (2).

(b) The reciprocal of the cotangent of the stator-exit angle. This function, described in (5), reflects the variation in the ratio of flow area to surface area.

(c) The average specific kinetic energy of the blade rows based on the entering and leaving velocities. This assumption is described in (5) where it was also assumed that the contribution of the rotor kinetic energy level to the loss was twice that of the stator. This assumption will be used in the subject development with the additional assumption that for an interstage stator between  $\lambda$  of 0 and 0.50 this weighing varies linearly from 2 to 1 to yield stator losses more consistent with experiment. Using  $f(\lambda)$  to denote this weighing function, the following is evident:

Rotor:

$$0 \leq \lambda \leq 1.00 \\ f(\lambda)_{ro} = 2$$

Stator - single or first stage:

$$0 \leq \lambda \leq 1.00 \\ f(\lambda)_{st} = 1$$

Stator - intermediate stage:

$$0 \leq \lambda \leq 0.50 \\ f(\lambda)_{st} = 2(1 - \lambda) \\ 0.50 \leq \lambda \leq 1.00 \\ f(\lambda)_{st} = 1$$

(22)

Fig. 4 presents a graphical representation of this function.

Using the assumptions described in the foregoing, the equation for  $L_{st} + L_{ro}$  can be written as

$$L_{st} + L_{ro} = \frac{K}{2gJ} \frac{(Re)^{-1/5}}{\cot \alpha_1}$$

$$\times \left[ f(\lambda)_{st}(v_0^2 + v_1^2) + f(\lambda)_{ro}(w_1^2 + w_2^2) \right] \quad (23)$$

and therefore using equation (21a) the equation for A becomes

$$A = K \frac{(Re)^{-1/5}}{\cot \alpha_1} [f(\lambda)_{st}C + f(\lambda)_{ro}D] \quad (24)$$

where

$$C = \frac{V_0^2 + V_1^2}{\Delta V_u^2} \quad (24a)$$

$$D = \frac{W_1^2 + W_2^2}{\Delta V_u^2} \quad (24b)$$

The relation between the parameters C and D and must still be determined.

**Parameter C.** To obtain the stator kinetic energy parameter C in terms of  $\lambda$  let the velocities in the numerator be split up into their components, Fig.1. This yields, when using the stator-exit axial component of velocity as representing the average,

$$C = \frac{2V_{x,1}^2 + V_{u,0}^2 + V_{u,1}^2}{\Delta V_u^2}$$

or

$$C = (1 + 2 \cot^2 \alpha_1) \left( \frac{V_{u,1}}{\Delta V_u} \right)^2 + \left( \frac{V_{u,0}}{\Delta V_u} \right)^2 \quad (25)$$

The value of  $V_{u,1}/\Delta V_u$  and  $V_{u,0}/\Delta V_u$  used depends upon the type diagram and therefore the level of  $\lambda$ . Using the relations of equation (7) and assuming in the case of the interstage stator that the whirl leaving the rotor ( $V_{u,2}$ ) is equal to that entering the interstage stator, the following equation for C is obtained:

Single or first stage:

$$0 \leq \lambda \leq 0.50$$

$$C = (1 + 2 \cot^2 \alpha_1) \left( \lambda + \frac{1}{2} \right)^2$$

$$0.50 \leq \lambda \leq 1.00$$

$$C = 1 + 2 \cot^2 \alpha_1$$

Intermediate and last stage:

$$0 \leq \lambda \leq 0.50$$

$$C = (1 + 2 \cot^2 \alpha_1) \left( \lambda + \frac{1}{2} \right)^2 + \left( \lambda - \frac{1}{2} \right)^2$$

$$0.50 \leq \lambda \leq 1.00$$

$$C = 1 + 2 \cot^2 \alpha_1$$

**Parameter D.** To obtain the rotor parameter D in terms of  $\lambda$  the numerator of equation (24b) is split up into velocity components as done for C. Thus,

$$D = \frac{2V_{x,1}^2 + W_{u,1}^2 + W_{u,2}^2}{\Delta V_u^2} \quad (27)$$

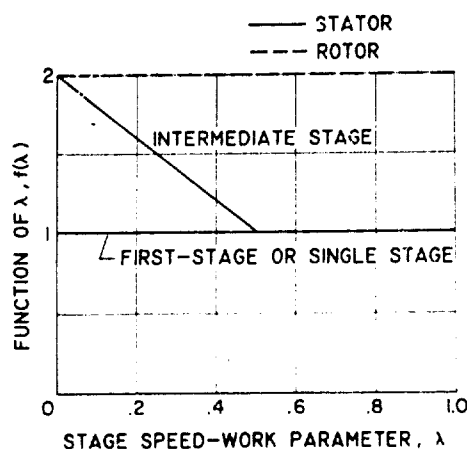


Fig. 4 Variation in  $f(\lambda)$  with  $\lambda$  as described in equation (22)

Now

$$W_{u,1} = V_{u,1} - U \quad (28)$$

and

$$W_{u,2} = V_{u,1} - U - \Delta V_u \quad (29)$$

Substituting equations (28) and (29) into equation (27) and using the definition for  $\lambda$  in equation (3) yield

$$D = 2 \cot^2 \alpha_1 \left( \frac{V_{u,1}}{\Delta V_u} \right)^2 + \left( \frac{V_{u,1}}{\Delta V_u} - \lambda \right)^2 + \left( \frac{V_{u,1}}{\Delta V_u} - \lambda - 1 \right)^2$$

Using equation (7) then yields

$$0 \leq \lambda \leq 0.50$$

$$D = 2 \cot^2 \alpha_1 \left( \lambda + \frac{1}{2} \right)^2 + \frac{1}{2}$$

$$0.50 \leq \lambda \leq 1.00$$

$$D = 2 \cot^2 \alpha_1 + (1 - \lambda)^2 + \lambda^2 \quad (30)$$

Thus the required expression for D is obtained.

**Reynolds Number.** In (6) it is shown that, although the Reynolds number based on mean camber length basically affects the momentum thickness, blade height is the better basis because of a series of counter-balancing effects on the loss as described in the reference. Therefore in this development the Reynolds number  $Re$  will be based on the blade height and in addition will be based on the velocity and density level leaving the stator:

$$Re = \frac{(\rho V)_1 l}{\mu}$$

The value of  $\mu$  will be taken to correspond to the turbine-inlet total conditions. If  $V_1$  is expressed in terms of  $V_x$  and  $\alpha_1$  and it is assumed that  $\alpha_1$  varies within sufficiently close limits

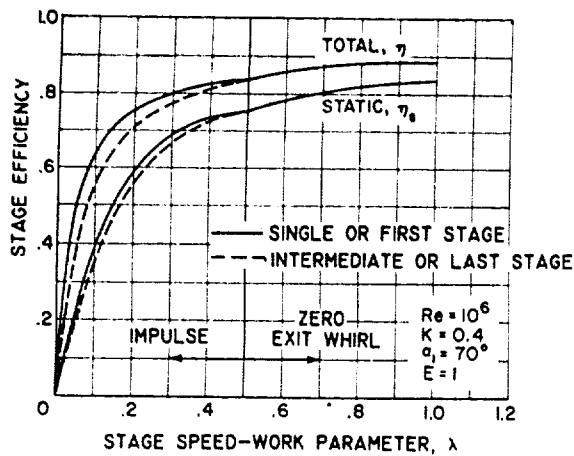


Fig. 5 Turbine-stage efficiency as a function of speed-work parameter

that the angle effect is relatively small, then

$$Re = \frac{(PV_x)_1}{\mu} \quad \frac{(PV_x)_1 2\pi r l}{2\pi r \mu}$$

Since  $2\pi r l$  is the annulus area, the following simplified definition is obtained and used in this paper:

$$Re = \frac{w}{\mu r} \quad (31)$$

The equation in this form can be used to represent the Reynolds number for the whole turbine regardless of number of stages.

#### Consideration of Stage Exit

##### Kinetic-Energy Loss Term B

The term B represents the contribution of the stage exit kinetic-energy to the turbine loss when the efficiency is rated based on total to static-pressure ratio. This term can be expressed in terms of  $\lambda$  by first splitting the numerator into its velocity components. Equation (21b) then becomes

$$B = \frac{V_{x,2}^2 + V_{u,2}^2}{\Delta V_u^2} \quad (32)$$

In general, the stage exit axial component of velocity is greater than that of the average represented by that at station 1. So defining

$$E = \left( \frac{V_{x,2}}{V_{x,1}} \right)^2 \quad (33)$$

and using it in equation (32) yield

$$B = E \left( \frac{V_{x,1}}{\Delta V_u} \right)^2 + \left( \frac{V_{u,2}}{\Delta V_u} \right)^2$$

Then introducing the stator angle  $\alpha_1$ ,

$$B = E \cot^2 \alpha_1 \left( \frac{V_{u,1}}{\Delta V_u} \right)^2 + \left( \frac{V_{u,2}}{\Delta V_u} \right)^2 \quad (34)$$

Introducing then the relations in equation (7), the following working relations are obtained

$$0 \leq \lambda \leq 0.50$$

$$B = E \cot^2 \alpha_1 \left( \lambda + \frac{1}{2} \right)^2 + \left( \lambda - \frac{1}{2} \right)^2 \quad (35)$$

$$0.50 \leq \lambda \leq 1.00$$

$$B = E \cot^2 \alpha_1$$

#### Summary of Equations Used

A review of the equations will be made in functional form to indicate the method used for computing the stage and over-all efficiencies as well as to indicate the required input information:

$$\bar{\eta}_s = f(N, \eta_a, \eta_1, \eta_{1,s}) \quad (17)$$

$$\eta = f(\lambda, A, B = 0) \quad (21)$$

$$\eta_s = f(\lambda, A, B) \quad (21)$$

$$A = f(K, Re, \alpha_1, C, D, f(\lambda)_{st}, f(\lambda)_{ro}) \quad (24)$$

$$B = f(E, \alpha_1, \lambda) \quad (35)$$

$$C = f(\lambda, \alpha_1) \quad (26)$$

$$D = f(\lambda, \alpha_1) \quad (30)$$

$$Re = f(w, \mu, r) \quad (31)$$

From these functional relationships the following are needed to make an efficiency calculation:

$$\left. \begin{matrix} w \\ \mu \\ r \end{matrix} \right\} Re$$

$$\lambda, \alpha_1, E, K, N$$

Since  $w, \mu$ , and  $r$  are used only to obtain  $Re$ , with  $Re$  used in the efficiency equations, then  $Re$  itself will be considered on the input variable in the analysis results section.

#### RESULTS OF STUDY

##### Stage-Efficiency Characteristics

Using the method just described for obtaining turbine efficiency for given diagram parameters, the stage-efficiency characteristics were first computed over the range of  $\lambda$  of interest (0 - 1.00) considering the other parameters constant. The value of  $K$  was selected as 0.4 since this value yielded analytical efficiencies that checked closely the experimental efficiencies obtained in the Transonic Turbine Program conducted at the laboratory [see (7), e. g.]. The stator-exit angle  $\alpha_1$ , Reynolds number  $Re$ , and exit axial energy parameter  $E$  were selected at representative values of  $70^\circ$ ,  $10^6$ , and 1.0 respectively.

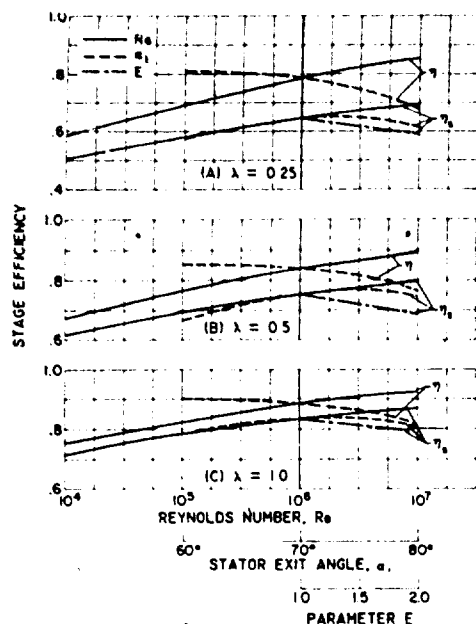


Fig. 6 Effect of  $Re$ ,  $\alpha_1$ , and  $E$  on efficiency at  $\lambda = 1.0$ ,  $K = 0.4$

The results of these calculations are shown in Fig. 5 where stage efficiency is presented as a function of the stage speed-work parameter  $\lambda$ . Considering first the total efficiency  $\eta$ , it is seen that at high values of  $\lambda$ ,  $\eta$  is quite high, 0.88 or greater at values of  $\lambda$  between 0.80 and 1.00. As  $\lambda$  is reduced to 0.50 (the limiting value for zero exit whirl)  $\eta$  reduces to approximately 0.84. In this range ( $0.50 < \lambda < 1.00$ ) the intermediate-stage curve coincides with the first-stage curve since their respective stators are identical. At  $\lambda = 0.50$  a break in the curve is seen to occur and results from the change from zero exit whirl conditions to that of impulse. Then as  $\lambda$  is reduced below 0.50, two curves form, the solid line representing a first or single stage, and the dashed line representing an intermediate or last stage. The single-stage curve is seen to reduce in value as  $\lambda$  is reduced below 0.50 with  $\eta$  becoming 0.75 at  $\lambda = 0.20$ . As  $\lambda$  is further reduced,  $\eta$  drops off very markedly, reaching 0 at  $\lambda = 0$ . As  $\lambda$  is reduced below 0.50,  $\eta$  for the intermediate stage starts to deviate downward considerably from the single-stage curve, being approximately 5 points lower at  $\lambda = 0.20$ . This difference in efficiency is, of course, due to the intermediate stators becoming considerably different from those of the first stage, having considerably more turning and lower reaction.

The stage static-efficiency characteristics are also shown in the figure. The general trends with  $\lambda$  are similar but at a lower level. This

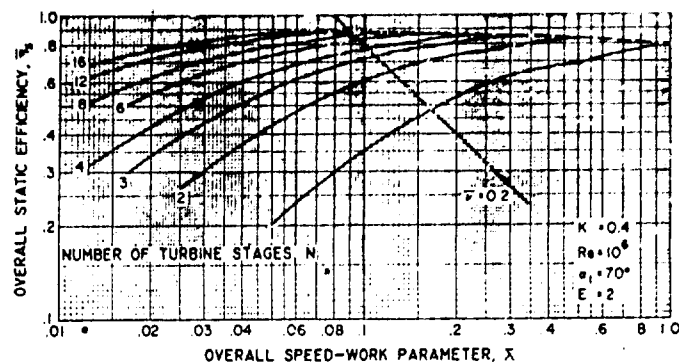


Fig. 7 Multistage turbine static-efficiency characteristics as a function of over-all speed-work parameter

of course is due to the leaving kinetic energy being considered a loss. The degree of difference is however considerably different for the zero exit whirl case as compared to that of impulse. In the range  $0.50 \leq \lambda \leq 1.00$  the efficiency difference is 5 to 8 points. In the impulse range as  $\lambda$  is reduced considerably below 0.5 this difference becomes much larger, being, for example, 17 points at  $\lambda = 0.20$  (single-stage case). This increasing difference is due to the increased required negative exit whirl out of the stage.

The effect of independently varying the Reynolds number, stator-exit angle, and stage-exit axial-kinetic-energy loss parameter on efficiency is shown in Fig. 6 for the case of the single-stage  $\lambda$  values of 0.25, 0.50, and 1.00. The solid vertical line in the figure represents the so-called base values of  $10^6$ ,  $70^\circ$ , and 1, respectively, such that the efficiency characteristics shown on this line coincide with those of Fig. 5.

The variation in stage efficiency with  $Re$  is shown over a range from  $10^4$  to  $10^7$  and shown for all parts of the figure a gradual reduction in both total and static efficiency as  $Re$  is reduced. This of course occurs because of the Reynolds number effect included in equation (24) for term A.

The effect of stator-exit angle  $\alpha_1$  on stage efficiency is shown over a range from 60 to 80 deg. It can be seen that for all  $\lambda$ -values considered the maximum total efficiency  $\eta$  occurs at an angle on the order of 60 deg with curves flat in this region. As the angles are increased beyond 70 deg,  $\eta$  starts to fall off markedly. The indication of an optimum angle occurs because of the two counterbalancing effects of the co-tangent angle function in equation (24) representing the effect of angle on the surface area per unit flow, and the angle functions in equations (26) and (30) representing the effect of angle



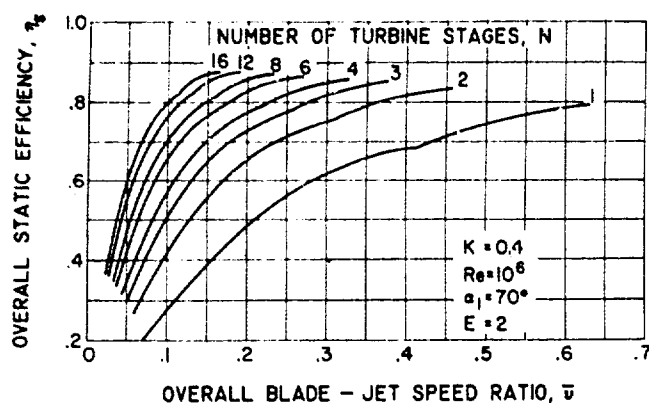


Fig. 8 Multistage turbine static-efficiency characteristics as a function of over-all blade-jet speed ratio

on the average kinetic energy level and therefore the loss per unit surface area. A similar optimum condition is seen to occur for  $\eta_s$  but shifting to a value of  $\alpha_1$  on the order of  $74^\circ$ . This large shift in optimum angle occurs because of the additional angle functions in equation (35) which reflect in the effect of angle on the stage axial component of leaving loss.

The effect of  $E$  on efficiency is shown over the range from 1 to 2. It is shown only for  $\eta_s$  since it enters only in equation (35) which affects this efficiency only. The efficiency is seen to drop off as  $E$  is increased and of course occurs because of the increased stage exit axial component of leaving loss.

#### Over-all Efficiency Characteristics

In order to illustrate the effect of stage number  $N$  on the over-all turbine-efficiency characteristics a set of calculations was made over a range of  $N$  from 1 to 16 using equation (17). Representative values of  $Re$ ,  $\alpha_1$ , and  $E$  were taken at  $10^6$ ,  $70^\circ$ , and 2, respectively. The value of 2 for  $E$  was selected since in general the turbine-exit axial kinetic energy is greater than the average. The results of the calculations are shown in Fig. 7, where the over-all static efficiency  $\bar{\eta}_s$  is presented as a function of the over-all speed-work parameter  $\bar{\lambda}$  over the range of stage number considered. The plot is presented on a log-log basis in order to separate the curves adequately in the low  $\bar{\lambda}$  range. An additional reason for plotting the curves on this basis will be described later.

Inspection of Fig. 7 shows that for a given number of stages  $N$  the trend of  $\bar{\eta}_s$  with  $\bar{\lambda}$  is essentially the same as that on a stage basis (compare with Fig. 5). The curves, however, are displaced toward lower  $\bar{\lambda}$ -values as the number of stages is increased. This occurs, of course,

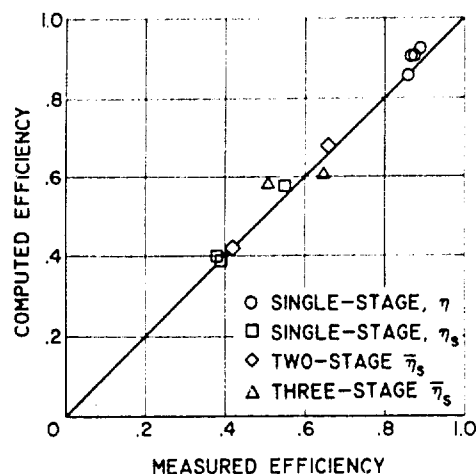


Fig. 9 Comparison between experimental and computed efficiency

because of the attainment of similar  $\bar{\lambda}$ -values and therefore comparable levels of  $\bar{\eta}_s$  at the lower  $\bar{\lambda}$  values when the additional stages are used. It can also be seen that in the high  $\bar{\lambda}$ -range ( $0.25 \leq \bar{\lambda} \leq 1.00$ ) only one or two stages are necessary for high efficiency. As  $\bar{\lambda}$  is reduced below this range, increased number of stages are required in order to keep the efficiency at a reasonable level. The dashed line shows the envelope of maximum  $\bar{\eta}_s$  that occurs at the point where  $\bar{\lambda} = 1.00$ . From this it follows that at this maximum efficiency point  $N = 1/\bar{\lambda}$  from equation (8).

As pointed out in the development section, another parameter, the blade jet speed ratio  $\bar{v}$ , is commonly used for correlating efficiency. This parameter is more meaningful from an operational standpoint in that the operating conditions, turbine speed and pressure ratio (uniquely specifying  $\bar{v}$ ), are imposed with efficiency and  $\bar{\lambda}$  being dependent. Since a relation between  $\bar{\lambda}$  and  $\bar{\eta}_s$  is established in Fig. 7, a relation between  $\bar{\eta}_s$  and  $\bar{v}$  can be obtained by using equation (12). Also from this equation it can be seen that  $\bar{v}$  is a function of the product  $\bar{\eta}_s \bar{\lambda}$ . Therefore a line of constant  $\bar{v}$  on Fig. 7 represents a curve of constant  $\bar{\eta}_s \bar{\lambda}$ . Since the plot shown is on a log-log basis, such a curve would be a straight line at a slope of -1. One such line is shown in the figure, that at  $\bar{v} = 0.2$ .

It can be seen that, to achieve a given increase in efficiency, a larger number of stages is required at a constant  $\bar{v}$  than at a constant  $\bar{\lambda}$ . This occurs because, if one considers a constant blade speed, an increase in efficiency at a constant  $\bar{\lambda}$  means at a constant actual specific work. On the other hand, at a constant  $\bar{v}$  with constant speed, the increase in efficiency

occurs at a constant ideal specific work. As a result, the actual specific work increases, requiring the additional stages to yield the same increment in efficiency.

The efficiency characteristics in Fig.7 are replotted in Fig.8 as a function of this blade-jet speed ratio. At  $\bar{v} = 0.2$  the correspondence in  $\bar{\eta}_s$  with that of the previous figure can be noted.

#### COMPARISON WITH EXPERIMENT

The method described in this paper was used to compute the design efficiency of a number of turbines that have been investigated experimentally at the laboratory in recent years. These turbines covered the following range of the diagram parameters used in this paper:

Re	$8 \times 10^4 - 4.6 \times 10^6$
$\alpha_1$	$55^\circ - 80^\circ$
E	1.3 - 1.8
$\bar{\lambda}$	0.06 - 0.97
N	1 - 3

A comparison of the experimentally obtained efficiencies with those predicted is presented in Fig.9 where computed efficiency is shown plotted against that measured. Both total and static efficiencies are shown since some of these turbines were of the turbojet type where total efficiency was measured, and others were of the turbo-pump and APU type where static efficiency was considered of most importance. From the figure it can be concluded that a reasonable agreement between the experimental and computed efficiency was obtained.

#### CONCLUDING REMARKS

This paper has presented the development of equations to be used in calculating the efficiency characteristics of axial-flow turbines in terms of their velocity diagram parameters. The check with available experimental data showed that the method was reasonably accurate in establishing this level. It might be noted again that the efficiency level is also a function of the design of the blading to meet these selected velocity

diagrams. The value of K selected was based on the performance of a turbine that had reasonably good surface velocity distributions with a resulting near-optimum solidity, close running and tip clearances, and small trailing edge blockages. The value of K would certainly become higher if the solidities and velocity distributions were nonoptimum, or if excessive running and tip clearances or large trailing-edge blockages were used. Such considerations should also be considered in the final selection of the design efficiency level.

Finally, the method described has been programmed for the IBM 704 computer at the laboratory. Anyone wishing a copy of this program or information on the programming method can feel free to contact the author.

#### REFERENCES

- 1 Warner L. Stewart, Warren J. Whitney, and Harold J. Schum, "Three-Dimensional Flow Considerations in the Design of Turbines," ASME Paper No. 59-HYD-1, 1959.
- 2 Warner L. Stewart, Warren J. Whitney, and Robert Y. Wong, "A Study of Boundary Layer Characteristics of Turbomachine Blade Rows and their Relation to Overall Blade Loss," ASME Paper No. 59-A-23, 1959.
- 3 A. Stodola, "Steam and Gas Turbines," McGraw-Hill Book Company, Inc., 1945.
- 4 Warner L. Stewart, "Analytical Investigation of Single-Stage-Turbine Efficiency Characteristics in Terms of Work and Speed Requirements," NACA RM E56031, 1956.
- 5 Warner L. Stewart, "Analytical Investigation of Multistage-Turbine Efficiency Characteristics in Terms of Work and Speed Requirements," NACA RM E57K22b, 1958.
- 6 James W. Miser, Warner L. Stewart, and Warren J. Whitney, "Analysis of Turbomachine Viscous Losses Affected by Changes in Blade Geometry," NACA RM E56F21, 1956.
- 7 Warner L. Stewart, Robert Y. Wong, and David G. Evans, "Design and Experimental Investigation of Transonic Turbine with Slight Negative Reaction Across Rotor Hub," NACA RM E53L29a, 1954.